



HAL
open science

Discovery of very active catalysts for methanol carboxylation into DMC by screening of a large and diverse catalyst library

C. Daniel, Y. Schuurman, D. Farrusseng

► **To cite this version:**

C. Daniel, Y. Schuurman, D. Farrusseng. Discovery of very active catalysts for methanol carboxylation into DMC by screening of a large and diverse catalyst library. *New Journal of Chemistry*, 2020, 44 (16), pp.6312-6320. 10.1039/c9nj06067g . hal-02639449

HAL Id: hal-02639449

<https://hal.science/hal-02639449>

Submitted on 2 Mar 2021

HAL is a multi-disciplinary open access archive for the deposit and dissemination of scientific research documents, whether they are published or not. The documents may come from teaching and research institutions in France or abroad, or from public or private research centers.

L'archive ouverte pluridisciplinaire **HAL**, est destinée au dépôt et à la diffusion de documents scientifiques de niveau recherche, publiés ou non, émanant des établissements d'enseignement et de recherche français ou étrangers, des laboratoires publics ou privés.



Distributed under a Creative Commons Attribution 4.0 International License

Discovery of very active catalysts for methanol carboxylation into DMC by screening of a large and diverse catalyst library

Cécile Daniel, Yves Schuurman, David Farrusseng*

IRCELYON, Institut de recherches sur la catalyse et l'environnement de Lyon,
Université de Lyon1, UMR CNRS 5256, 2 Avenue Albert Einstein, Villeurbanne F-
69626, France

Keywords: ceria, zirconia, flame spray pyrolysis, DMC, CO₂

Abstract

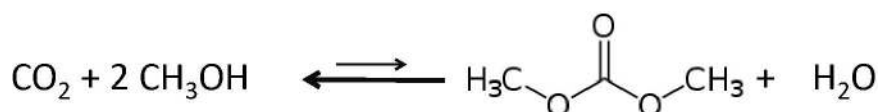
The direct synthesis of dimethyl carbonate from methanol and CO₂ is particularly attractive as it provides a green alternative to other routes while allowing CO₂ conversion. Although the evaluation of catalyst formulations figures prominently in the literature, one can hardly identify which formulations are the most active. One of the reasons is that there is no standard testing protocol. Initial water content in the reactive mixture is critical as it can drag down thermodynamic equilibrium. This study aims to rank catalyst activities and to identify the most active catalysts using a systematic protocol for the measurement of the true catalytic activity. Based on an assessment of critical parameters, a protocol for the measurement of the activity in the liquid phase, taking care to the limitation induced by thermodynamic equilibrium, was developed. Special attention was paid to the quantitative assessment of critical experimental parameters. Following the protocol, a screening of various pure and mixed oxides of about 60 different solids was carried out. Finally, an optimization

study was carried out on Zr-Ce mixed oxides produced by different synthesis methods, leading to the discovery of the catalyst which, to the best of our knowledge, is the most active reported so far.

1 Introduction

Among organic carbonates, dimethyl carbonate (DMC) is a promising green chemical because of its low toxicity and rapid biodegradability¹². Its versatile chemical properties account for its wide use as an agent in carbonylation and methylation reactions, replacing DMSO, COCl₂ and CH₃X³⁴. It is also largely used as a precursor for the production of polycarbonates and polyurethanes. DMC offers excellent solvating properties and is therefore used as a safe solvent in organic synthesis⁵. It has a high oxygen content (53%) and is a promising oxygenate additive to gasoline, compared to other chemicals such as MTBE, ethanol or methanol⁶. Due to its high dielectric constant, DMC is used as an electrolyte in lithium-ion batteries⁷.

DMC was historically synthesized by the harmful methanolysis of phosgene. Current industrial processes include the hazardous, corrosive oxidative carbonylation in gas or in liquid phase⁸. Other possible routes are transesterification of propylene carbonate and methanolysis of urea^{9 10}.



The direct synthesis of DMC from methanol and CO₂ (reaction 1) appears particularly attractive: it is a greener alternative to the other routes that simultaneously allows CO₂ valorization¹⁰. However, the methanol conversion, X_{MeOH} , is strongly limited by thermodynamic equilibrium. The standard Gibbs enthalpy was evaluated at 26 kJ.mol⁻¹^{11, 12}. As a consequence, the DMC yield, assuming 100% selectivity, can hardly exceed 2% even at favorably high pressure¹³ and at temperatures below 473K.

Dehydration of reactive media can be used to increase the DMC yield. Several researchers have used *in situ* reactive water traps such as trimethyl phosphate, butylene oxide¹⁴, acetonitrile¹⁵ and 2-cyanopyridine¹⁶, reaching per-pass yields of up to 6%. The use of an inorganic water trap such as zeolite

3A in a multi-pass process yields up to 40% DMC¹⁷. Recent studies demonstrate that a direct synthesis process can technically achieve high DMC yield, when an efficient dehydration process is applied. With this in mind, the application of catalytic membrane reactors allowing continuous water withdrawal during reaction has also been proposed, and a successful proof of concept was recently reported^{18 19}.

A large diversity of catalysts have already been tested for the direct synthesis of DMC^{20 21}, including organic metal-alkoxy compounds, metal oxides, metal-supported catalysts and ionic liquids. It is generally proposed that well-balanced acidic and basic properties play a key role in DMC synthesis for methanol activation^{22 23 24}. The majority of metal oxide studies deal with ceria or zirconia^{25 26 27}. The effects of crystal structure and morphology on activity are still under debate. Ceria catalysts exhibiting nanorods, nanocubes, octahedrons and spindle-like morphologies show different activities^{28 29 30}. Generally, the observed tendency is that mixed oxides often perform better than pure oxides. Hence, authors have explored modified ceria and zirconia such as H₃PO₄-functionalized ZrO₂^{23 31}, ceria doped with Al₂O₃, Fe₂O₃^{32 33}, as well as mixed oxides of ceria – zirconia^{24 34 22 35 36}. Although many catalyst formulations have been evaluated in the literature, one can hardly identify which formulations are the most active. One of the reasons is that because no standard testing protocol has been established, the processes developed have been very diverse. Several studies have been carried out in the gas phase in a fixed-bed reactor at low pressure, enabling continuous withdrawal of water, and therefore conversion beyond thermodynamic equilibrium. Most of the measurements are carried out under pressure in the liquid phase in batch reactors, resulting in very low conversion (<2%) limited by thermodynamic equilibrium. Remarkable differences in yields for both processes are reviewed in³⁷. Unfortunately, most of the studies do not report catalytic activities, i.e., moles converted per unit of time and catalyst mass, but only conversion data. Moreover, data measured at conditions close to thermodynamic equilibrium cannot be used to calculate the catalytic activity. In addition, the equilibrium conversion is difficult to calculate due to the lack of accurate thermodynamic data under reaction conditions that are often non-ideal and the fact that traces of water, notably those contained in the solid catalyst, have a strong impact on the equilibrium. Unfortunately, this last issue has been neglected in most studies^{38 39}. Finally, water formed during the reaction may cause the deactivation of some catalysts⁴⁰. As a conclusion, a ranking of catalytic activities across the literature can hardly be established on a rational basis. This is true, for example, for pure cerium oxides, one of the most studied catalysts^{28 29 30 41}.

This study aims to rank catalyst activities and to identify very highly active catalysts using a systematic process allowing the measurements of “true” catalytic activities. Based on an assessment of critical protocol parameters, a protocol for the measurement of catalytic activity far from equilibrium was developed, with special attention paid to critical experimental parameters. Following this protocol, a

screening of different pure and mixed oxides was carried out. Finally, an optimization study was carried out on Zr-Ce mixed oxides obtained from different synthesis methods, leading to the discovery of the catalyst which, to the best of our knowledge, is the most active reported so far.

2 Experimental

2.1 Catalyst sourcing and preparation

In total 61 catalysts were tested. The list of catalyst formulation and catalytic activities is available in Supporting Information.

Pure oxides were purchased from Sigma Aldrich, Fluka, Acros and Alfa-Aesar. Other samples were synthesized using three different synthesis procedures described below.

Co-precipitated mixed oxides referenced as **CP-** were prepared from nitrate salt precursors. Predetermined amounts of salts were mixed in aqueous solutions and added dropwise to a solution of NaOH heated at 333K. The precipitate was washed until conductivity dropped below 50 μ S. The final sample was calcined under air at 773K for 5 h. Pure zirconia and pure ceria used to prepare impregnated samples, referenced as **P-ZrO₂** and **P-CeO₂**, respectively, were synthesized according to the same single precipitation method. Mixed co-precipitated oxides were labeled **A_xB_{1-x}O₂**, where A= Ce or Zr, B=Al, Gd, Nb, Ti, Fe, La or Zr, and x stands for the molar fraction of A.

Pure zirconia, pure ceria and zirconia-ceria mixed oxides were also prepared by flame spray pyrolysis, referenced as **FSP**. The typical equipment and synthesis parameters are described elsewhere^{42 43}. The powders obtained were calcined under air at 773K for 5 h. The molar composition is noted **A_xB_{1-x}O₂**.

Finally, a third series of catalysts was prepared by impregnation of ceria **P-CeO₂** with a second metal M in solution and calcined at 773K under air for 5 h. They were labeled as **z % M/CeO₂**, where M is the impregnated metal and z the targeted weight percentage.

2.2 Catalyst Characterization

The surface area was calculated by the Brunauer-Emmett-Teller (BET) method from N₂ physisorption isotherms using a Belsorp Mini instrument (Bel Japan). Before N₂ physisorption, the samples were heated at 473K for 3 h in a vacuum ramp (Belprep, Bel Japan).

Powder X-ray diffraction patterns (XRD) were recorded to assess solid crystallinity. Diffractograms were collected between 4 and 90° (2 θ) with steps of 0.02° and 1 s per step with a Bruker D8 Advance A25 diffractometer using Cu K α radiation at $\lambda = 1.5418 \text{ \AA}$. The average crystallite size was calculated using the Scherrer method.

Elemental analysis of the catalysts was performed using an ICP-OES (Inductively Coupled Plasma-Optical Emission Spectrometry) ACTIVA from HORIBA Jobin Yvon equipped with a CCD detector for the determination of metal loadings.

2.3 Method of carboxylation of methanol and CO₂

Anhydrous methanol was purchased from Carlos Erba with a water content below 300 ppm. Anhydrous toluene was purchased from Sigma-Aldrich with a water content below 10 ppm. Liquid CO₂ was supplied by Messer with a purity of 99.995% and a water content below 5 ppm.

The three-phase catalytic carboxylation of methanol was carried out in a high-pressure Parr Instrument vessel of 50 ml volume equipped with a pressure indicator, used as a batch reactor. Typically, an adjusted amount of dried catalyst in powder form (ranging from 20 mg to 500 mg) and 12 g of methanol with 0.1 wt % anhydrous toluene as internal standard were introduced into the vessel. The reactor was purged 3 times with 10 bar of dry N₂. A volume of 18 ml of liquid CO₂ kept at 281K and 50 bar was fed to the autoclave with an Isco 250D syringe pump. The reactor was heated in an oil bath at 413 K for 4 h, under magnetic stirring. We observed that the rate at which CO₂ was introduced had an effect on the final pressure. The dissolution of CO₂ into methanol is rather slow as it takes several minutes. As a result, the final amount of dissolved CO₂ depends on the feeding rate. Consequently, in order to obtain a reproducible final pressure, the same CO₂ feeding rate and feed duration were applied by means of a syringe pump. In our protocol the vessel reached a stable pressure of 120 bar after 1 hour of reaction (Table 1S).

Under such conditions, the reaction takes place in the liquid phase with the suspended catalyst, which is in equilibrium with the vapor phase. The reaction was stopped after 4 hours by cooling the vessel in an ice bath. An aliquot from the liquid phase was sampled through a 0.45 μm filter (Millipore) in order to remove powder catalyst. We have analyzed by GCMS the composition of the liquid phase after reaction (Shimadzu QP 2010 GCMS equipped with a ZB Wax column). The only product of the liquid phase is DMC. In addition no DME could be noticeable in the gas phase after reaction carried out with P-CeO₂ and P-ZrO₂, the later being acid catalyst. As consequence, we do not expect production of DME with other oxides screened in the test conditions applied here and gas phase was not systematically analyzed.

Reaction products were quantified by an Agilent GC 6850 equipped with a capillary column DB WAXetr (30 m) and a flame ionization detector. The GC detection limit of DMC was evaluated at 0.015 wt %. Each value referring to conversion is evaluated on methanol basis.

The catalyst activity was calculated on the basis of the amount of DMC produced after 4 hours of reaction with an initial molar ratio $\text{MeOH}/\text{CO}_2=1$ at $T=413 \pm 2$ K, and $P=120 \pm 2$ bar and expressed as the number of moles DMC produced per gram of catalyst per second. In contrast to most studies in which activities are calculated with methanol-based conversions approaching thermodynamic equilibrium, the amount of catalyst in this study was adjusted to always keep the conversion below 0.6%. For example, the catalyst loading was 500 mg and 20 mg for the least and most active samples, respectively, while all other testing parameters were kept constant.

The water content was checked by coulometric Karl Fischer titration with a Titrando 905 Methrom apparatus. Hydranal Coulomat (Sigma Aldrich) was used for titration.

3 Results and discussion

3.1 Determination of equilibrium conversion and repeatability

The presence of water in the reaction mixtures interferes with the catalytic measurements in different ways. First of all, the reaction produces water and the equilibrium conversion under typical reaction conditions is very low, i.e., 0.7% on a dry basis (see details in E.S.I.). When measuring the catalytic activity, the conversion needs to be sufficiently below the equilibrium conversion to neglect the effect of the reverse reaction on the catalytic activity. An accurate estimation of the equilibrium conversion is thus necessary and requires knowledge of the initial water content. Water can also inhibit the reaction rate by chemisorption on the active sites in competition with methanol chemisorption on the same sites. A variation of the initial water content might lead to a variation of the catalytic activity, so it is important that all samples are evaluated under the same conditions. Further detailed kinetic studies will be necessary to reveal this inhibition effect. Finally, water might lead to catalyst deactivation. Therefore, the different origins and quantities of the introduction of water into the reaction mixture were evaluated.

Assuming the presence of 300 ppm of water in methanol and 5 ppm in CO_2 , the initial water content represents less than 10% (0.002 g) of the expected water production by reaction assuming a conversion

of 0.7% on a dry basis (0.0236 g) (details in SI). Another possible source of water contamination can be physisorbed water on the catalyst if it is not properly dried prior to catalytic measurements; this may represent up to 30% of the expected water production (see E.S.I. Table 2S). In light of these preliminary estimations, all catalysts were desorbed at 473K under primary vacuum in our protocol. A fresh bottle of methanol was used at each catalytic run. The water concentration was always below 300 ppm (Karl Fischer measurements).

As already stated, because of the lack of accurate thermodynamic data for the given operating conditions and the fact that water content has a strong impact on the equilibrium conversion, the conversion at thermodynamic equilibrium was experimentally measured. Conversion measurements were carried out with four different catalysts at 413K and 120 bar for an initial MeOH:CO₂ ratio of 1 and an estimated initial water content of 300 ppm. Conversion was measured after 24 hours of reaction, which is six times longer than the time period used for activity measurements. The conversion at thermodynamic equilibrium (X_{eq}) was found to be near 0.8% \pm 0.02 (sd) for the four catalysts and is therefore catalyst independent as expected (Fig. 1). The value of 0.8% was taken as the thermodynamic equilibrium, which is in good agreement with literature data between 413 and 443K^{39 26}.

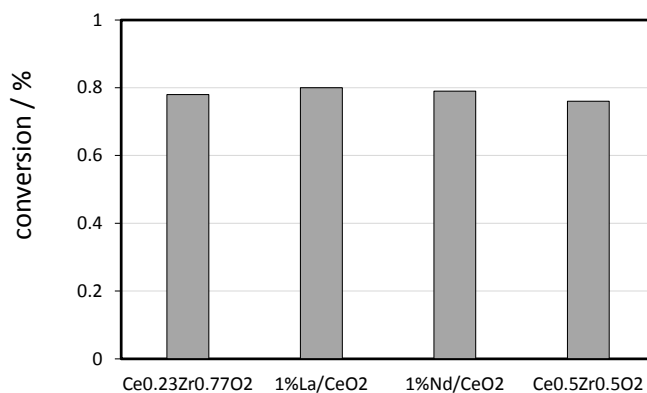


Fig. 1: Evaluation of conversion at thermodynamic equilibrium for the set of conditions: 413K, 120 bar, ratio MeOH:CO₂:1:1, t=24 h, W_{cat}=0.5 g, batch operation.

The reaction conversion as a function of time was followed over 48h over CP-Ce_{0.63}Zr_{0.37}O₂ (see E.S.I. Fig 4S). The initial rate of reaction was found to be linear until 4h. According to this result, the reaction time was set at 4 hours for the screening protocol which was used to measure the catalytic activity of the catalyst library. The stirring rate was not found to influence catalytic activity measurements. Increasing the stirring rate from 1500 rpm to 2000 rpm did not change results in the conditions described in Fig. 2.

A repeatability study of the activity measurement protocol was carried out through 10 identical runs over the same catalyst. We established an average conversion of $0.29\% \pm 0.02$ (sd), corresponding to a relative error of $\pm 7\%$ that has been applied for the calculation of activities.

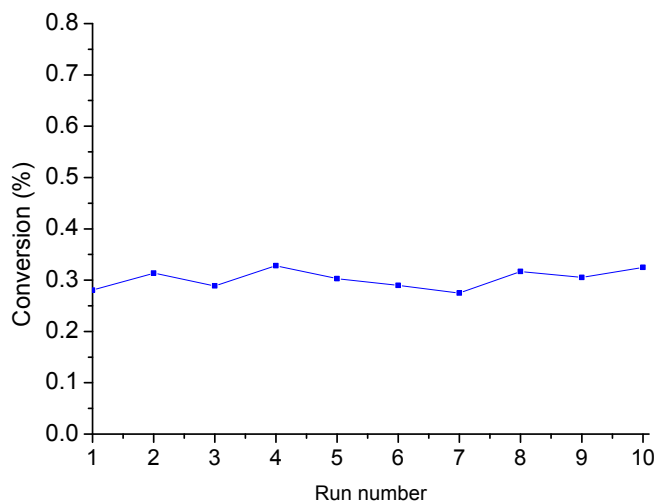


Fig. 2 : Repeatability of conversion over CP-Ce_{0.63}Zr_{0.37}O₂ at 413K for 4 h, molar ratio MeOH/catalyst =577 mol/mol. P=120 bar, MeOH:CO₂=1:1, Wcat= 0.1 g.

3.1.1 Library of pure oxides

Commercial oxides were selected to complement literature results covering different acid-base scales according to ⁴⁴ ⁴⁵. These commercial oxides were revealed to have low specific surface areas below 10 m²g⁻¹. Among all oxides tested, only ceria and zirconia were active. CeO₂ and ZrO₂ were fully selective in DMC synthesis. No other by-products, such as DME, were found.

Table 1 : Activity of pure oxides for direct synthesis of DMC

Oxide	Properties	Activity @413K μmol DMC.g ⁻¹ .s ⁻¹	S BET m ² .g ⁻¹
TiO ₂	Amphoteric	0	7.5.
La ₂ O ₃	Lanthanoids, Basic	0	5.2
Pr ₆ O ₁₁	Lanthanoids, Basic	0	4
Nb ₂ O ₅	Acidic	0	0.5
SrO	Basic	0	2.6
Gd ₂ O ₃	Lanthanoids, Basic	0	2
Ga ₂ O ₃	Amphoteric	0	11
ZnO	Amphoteric	0	7.5

CeO ₂	Lanthanoids, Basic	<0.01	7
ZrO ₂	Acidic	<0.01	3

3.1.2 Pure ceria

Various ceria sources with different specific surface areas and particle size distributions were evaluated from commercial suppliers. Synthesis methods of commercial oxides are unknown. All ceria samples were active in DMC synthesis and fully selective.

Table 2: Activity and specific surface areas of various ceria.

Entry	Ceria sample	Specific surface area (m ² .g ⁻¹)	Activity (μmol.g ⁻¹ .s ⁻¹)
A	Ceria 1 (Johnson Matthey)	100	0.51
B	Ceria 2 (Johnson Matthey)	135	0.25
C	Ceria 3 flame spray pyrolysis (Johnson Matthey)	99	0.31
D	Ceria precipitated	115	0.38
E	Ceria HSA (Solvay)	237	0.2
F	CeO ₂ Aldrich nanopowder (particle size < 25 nm)	30	0.16
G	CeO ₂ Aldrich microsized (particle size < 5 μm)	20	0.03
H	CeO ₂ fused (3-6 mm pellets)	2	0.01

Although only ceria is concerned, no clear relation can be established between the activity data and the specific surface area (see Figure 1S in E.S.I). On one hand, low specific surface area samples below 50 m².g⁻¹ generally exhibited poor activity. But on the other hand, high specific surface area alone is not sufficient for high activity, as demonstrated by the sample with a surface area of 237 m².g⁻¹ (entry E), but an activity of only 0.2 μmol.g⁻¹.s⁻¹. Yoshida et al. have concluded that high crystallinity of ceria calcined below 873K is a favorable property for catalytic activity⁴⁶. Different morphologies of ceria such as nanorods, octahedrons and nanocubes were also used to produce DMC³⁰. The authors concluded that the crystal planes as well as the number of acid and basic sites are decisive factors for active DMC catalysts. Hence, the difference in surface properties and crystal defects may explain the difference in activity observed in Table 2 for the pure ceria samples.

3.1.3 Ceria mixed oxides and zirconia mixed oxides

Impregnation method

A series of ceria mixed oxides was prepared by impregnation of a second metal followed by a thermal treatment. The initial pristine ceria (noted P-CeO₂), was prepared by precipitation and provided by

Johnson Matthey. The addition of a second metal (Al, Zn, Fe, La, Y, Gd, Sm, Zr, Nd) was carried out by a wetness impregnation process to reach a loading between 1 -5 wt.%. After heating the sample at 773K in air, the surface area of the serie ranged from 85 to 97 m² g⁻¹ were obtained, which was 15 to 25% lower than the surface of the pristine ceria material. Two additional catalysts were prepared by adding a second thermal treatment at 1023K in air on 1% Al/CeO₂ and 5 % La/CeO₂.

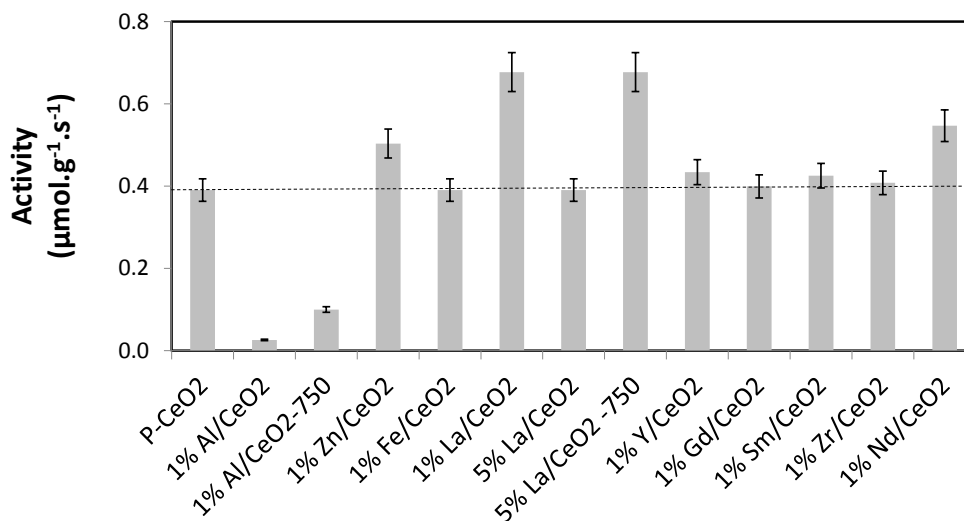


Fig. 3: Activity of ceria mixed oxides obtained by impregnation-heat treatment. Except for those noted with the label -750, all samples were heat-treated at 773K in air. P-CeO₂ is pristine ceria before impregnation. The horizontal dashed line is a guide for the eyes.

Taking the activity of precipitated pristine ceria (P-CeO₂) as a benchmark, we can define metal additives that do not change the activity, that improve the activity or that on the contrary are detrimental. Obviously, ceria impregnated with Fe, Y, Gd, Sm or Zr oxides and treated at 773K did not show any significant effect on the activity with respect to the pristine ceria. We want to stress here that we do not conclude that the addition of one of these metal oxides using a different synthesis procedure may not lead to higher activities. Indeed, as we will show below, Ce-Zr mixed oxides obtained by other means are much more active. Impregnation with Al made the activity drop dramatically, despite a high measured specific surface area of 85 m².g⁻¹. This might be due to coverage of active ceria sites by a layer of amorphous alumina. Nevertheless, even a five-hour thermal treatment at 1023K for 1 wt.% Al/CeO₂, which could have led to a better alumina dispersion, did not improve the performance, although its specific surface area remained high (52 m².g⁻¹).

The observed trend indicates a significantly enhanced activity in the following order: La > Nd = Zn. The increase of the La loading from 1 wt.% to 5 wt.% results, however, in a loss of the activity. On the other hand, the activity of 5 wt.% La/CeO₂-750 is surprisingly boosted after a thermal treatment at 1023K despite a reduced specific surface area of 63 m² g⁻¹.

Ceria and zirconia mixed oxides prepared by co-precipitation with a second metal oxide

All mixed oxides prepared by co-precipitation were nanocrystalline with a crystallite size between 4 and 8 nm (estimated by the Debye-Scherrer method) and specific surface areas (BET method – N₂) ranging from 90 to 130 m² g⁻¹ (see Table 5S, E.S.I). XRD analysis showed that cerium-based oxide was crystallized in a cubic structure, whereas zirconia-based samples had a tetragonal structure (Fig. 2S and Fig. 3S).

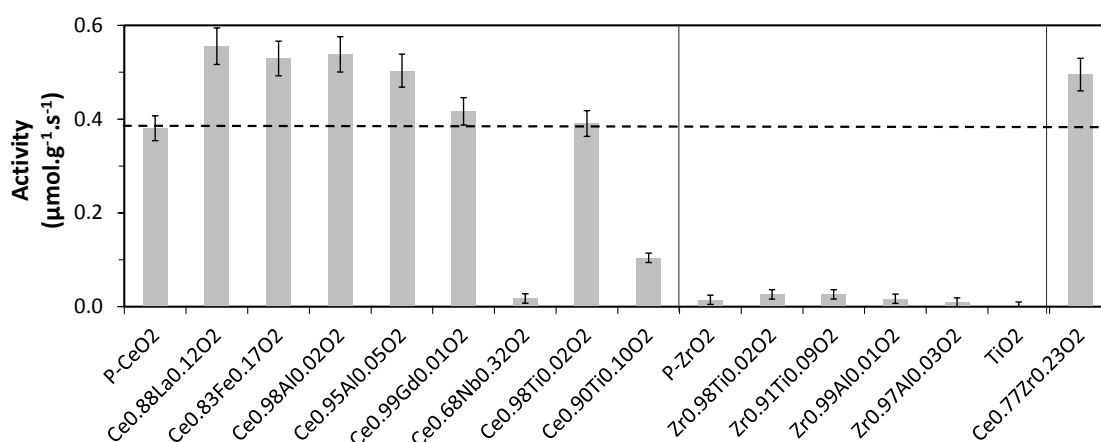


Fig. 4: Catalytic activity of co-precipitated Ce- and Zr-mixed oxides (composition in molar composition). The horizontal dashed line that corresponds to the activity of P-CeO₂ is a guide for the eyes.

At a first glance, ceria-based catalysts prepared by co-precipitation are more active than zirconia-based samples. For zirconia-based catalysts obtained by co-precipitation, namely Zr_{0.98}Ti_{0.02}O₂, Zr_{0.91}Ti_{0.09}O₂, Zr_{0.99}Al_{0.01}O₂, Zr_{0.97}Al_{0.03}O₂, we can hardly identify which metal oxides have a positive or negative effect due to the very low activity. We can observe that the Al- or Fe-containing oxides increased the activity of about 20%, in agreement with Aresta et al. who have reported higher activity for mixed oxides, namely 3-10 wt.% Al/CeO₂^{32 33} and 7 wt.% Fe/CeO₂ prepared by co-precipitation.

The co-precipitation with niobium oxide inhibited the activity, suggesting that large amount of Nb is not favorable to DMC synthesis⁴⁷. A 10 wt.% concentration of titanium oxide decreases the catalytic activity, whereas a low incorporation (2 wt.%) has no significant effect.

3.1.4 Third generation: ceria-zirconia mixed oxides by co-precipitation and flame spray pyrolysis

A number of literature studies have highlighted high activities of mixed ceria-zirconia samples^{22 31 34 35 36}. However, the effect of the mixing is not obvious with respect to the pure oxides, as both are active. In addition, we show here that the synthesis of mixed oxides by post-impregnation of zirconium oxide precursor on cerium oxide does not improve the catalytic activity (Fig 3) whereas co-precipitation leads to a synergistic effect (Fig 4). Apparently, the preparation method is a key parameter for obtaining very active ceria-zirconia catalysts. Therefore, we decided to complete the screening of ceria-zirconia catalysts prepared by co-precipitation (CP) by investigating the effect of the composition range from pure ceria to pure zirconia and the effect of the heat-treatment temperature from 423 to 1123K. In addition, we have explored the catalytic activities of ceria-zirconia catalysts prepared by flame spray pyrolysis. In order to compare catalytic results between CP and FSP synthesis methods, we have targeted the same molar composition (noted x hereafter) and the same treatment temperatures were applied.

Co-precipitated mixed oxides

Co-precipitated mixed oxides are true nanocrystalline solid solutions as far it can be determined by XRD (see Fig 2S). The surface areas of the solids obtained ranged from 87 to 126 m² g⁻¹, for crystallite sizes between 3.6 and 8 nm (see E.S.I Table 6S).

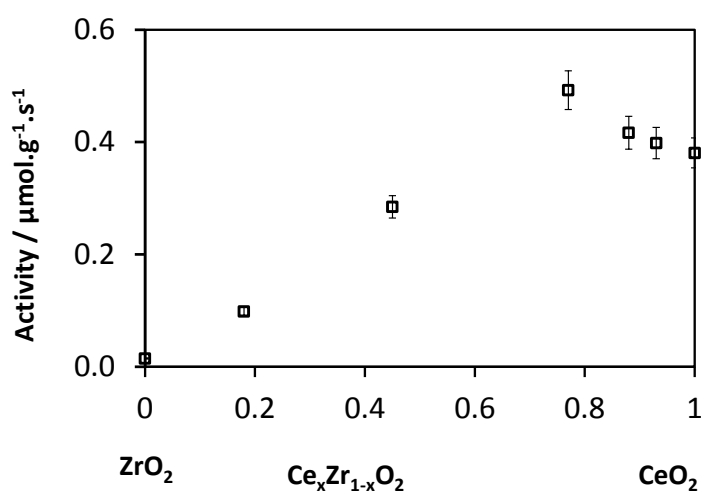


Fig. 5: Activity of $Ce_xZr_{1-x}O_2$ prepared by co-precipitation and calcined at 773K.

The activities of $Ce_xZr_{1-x}O_2$ mixed oxides prepared by co-precipitation and calcined at 773K are presented in Fig. 5. Interestingly, all intermediate compositions were more active than the pure oxides CeO_2 and ZrO_2 , i.e., there is a clear synergistic phenomenon. The maximum of activity is reached for the composition $Ce_{0.77}Zr_{0.23}O_2$ ($x=0.77$). These results are in good agreement with previous studies showing that the catalytic activity strongly depends on the Ce/Zr ratio. In ²² the authors prepared $Ce_xZr_{1-x}O_2$ by a sol-gel method and calcined the catalysts at 773K. The amount of DMC produced showed a “volcano-shaped” curve with respect to the cerium content, with a maximum at $x=0.6$ corresponding to $Ce_{0.6}Zr_{0.4}O_2$. Another study found the same composition-activity profile with the highest activity for $Ce_{0.5}Zr_{0.5}O_2$ prepared by a citric acid sol-gel method ⁴⁸. However, for reasons that are unknown to us, the activity of the latter is about one order of magnitude lower.

The co-precipitated $Ce_{0.88}Zr_{0.12}O_2$ was selected for optimization by post-thermal treatment. We observe, as expected, a decrease of the surface area upon increasing the temperature that is due to sintering (Fig. 6). Unexpectedly, the activity follows the opposite trend, i.e., it increases when the treatment temperature increases, resulting in an anti-correlation between the activity and the surface area. Although the specific surface area drops below $40\text{ m}^2\cdot\text{g}^{-1}$ with a thermal treatment at 1123K, the activity remains high at $0.4\text{ }\mu\text{mol g}^{-1}\text{ s}^{-1}$. A similar temperature-dependence trend of the activity was reported for $Ce_{0.3}Zr_{0.7}O_2$ ²⁴.

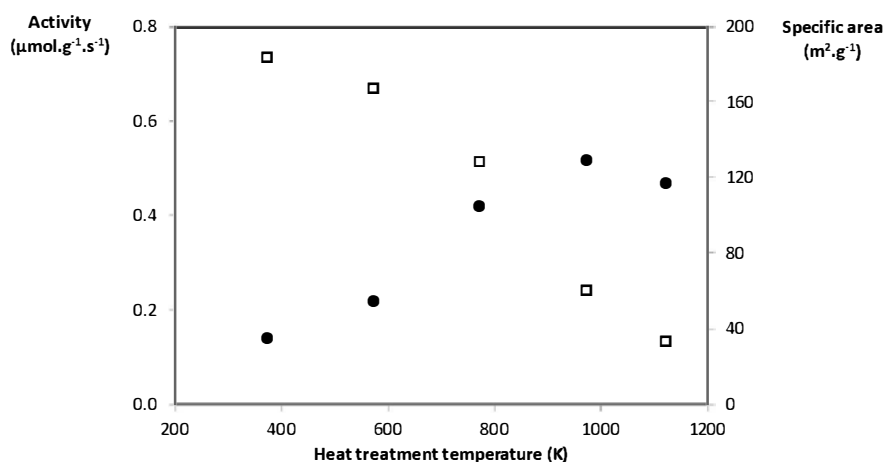


Fig. 6: Evolution of the activity (●) and surface area (□) of $Ce_{0.88}Zr_{0.12}O_2$ prepared by co-precipitation as a function of the temperature treatment.

Flame spray pyrolysis ceria-zirconia

In good agreement with previous studies ^{49 50} the characterization of flame spray pyrolysis ceria-zirconia samples revealed solid solutions with specific surface areas between 88 and 99 m² g⁻¹ and crystallite sizes between 6 and 10 nm (E.S.I Table 7S).

The flame spray pyrolysis ceria-zirconia were about one order of magnitude more active than the corresponding co-precipitated solids of the same composition. Whereas the studies of co-precipitated ceria-zirconia were carried out using 0.1 g of solid, the amount of catalyst was adjusted down to 0.02 g for the flame spray pyrolysis samples, otherwise the equilibrium conversion would have been reached well before the sampling time (see section 3.1.3).

The activities of flame spray pyrolysis ceria-zirconia as a function of the composition are compared to the co-precipitated (CP) solids (Fig. 7). The activity profile follows a “volcano” curve as reported above and is similar in trend to the co-precipitated samples. However, we cannot define here which composition corresponds to the highest activity, because the region with 0.5 < x < 1 was not experimentally investigated. Nevertheless, we can assume from the shape of the curve and the trend of the co-precipitated ceria-zirconia oxide that the maximum activity should be found in the region of equimolar Zr:Ce composition (x=0.5).

Astonishingly, the activity of the FSP mixed oxide Ce_{0.5}Zr_{0.5}O₂ (x=0.5) reached an activity of 6 μmol g⁻¹ s⁻¹, which is 20 times higher than that of the CP mixed oxide with the closest molar composition (x=0.45). FSP zirconia was six times more active than precipitated zirconia, whereas the difference in activity was negligible for pure ceria.

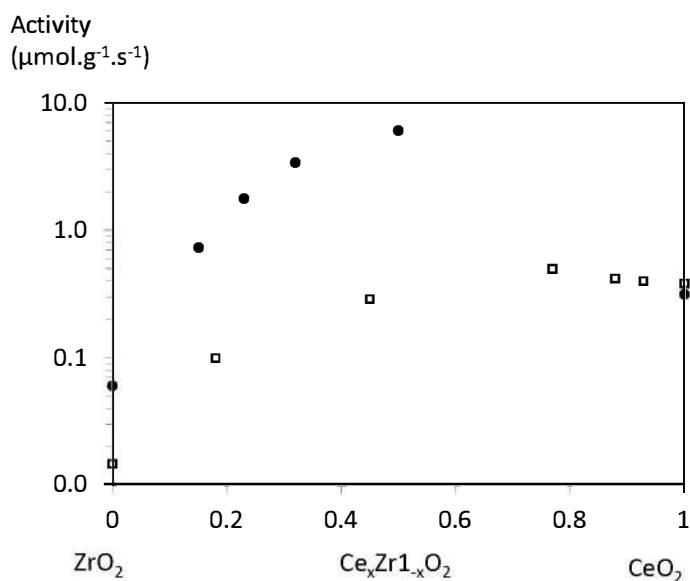


Fig. 7: Comparison of catalytic activities of flame spray pyrolysis Ce_xZr_{1-x}O₂ compared to co-precipitated solids. The activity scale is presented as a log scale. FSP: ●, CP: □

The X-ray diffraction patterns of co-precipitated and flame spray pyrolysis ceria-zirconia are compared in the SI (Fig 2S and 3S). For each set of catalysts, the continuous shift of the patterns versus the molar composition indicates that both CP and FSP series are solid solutions of ceria-zirconia. Although the XRD is not accurate enough to draw a conclusion regarding the homogeneity of the solid solution at nanoscale level, we cannot see a significant structural difference in the bulk phase⁵¹. Hence, the crystallite sizes of CP and FSP (Debye-Scherrer) are in the same range (E.S.I Table 6S, 7S). The specific surface area of whole CP and FSP mixed oxides vary relatively little (from 93 m² g⁻¹ up to 126 m² g⁻¹). In contrast, the catalytic activity varies by more than an order of magnitude across the CP and FSP mixed oxides. Such a difference in activity cannot be the result of a different number of the same active sites and should originate from a different kind of active sites. A more detailed investigation of the crystalline structure and the surface properties by complementary techniques is required to postulate a possible relation between structural features and the catalytic activity. This study goes well beyond the scope of this paper and will be published elsewhere.

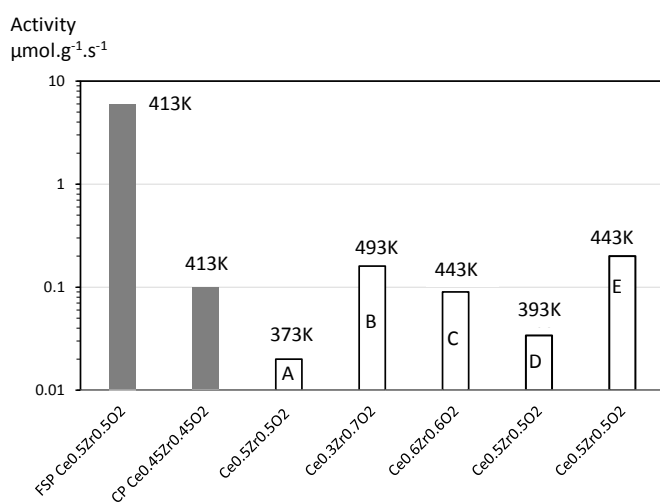


Fig. 8: Comparison of catalytic activities in log scale of ceria-zirconia mixed oxides with an equimolar composition or nearly equimolar composition from this study and compared with literature data A: ⁴⁸; B: ²⁴; C: ²²; D: ³⁴; E: ³⁵. For each condition, the temperature is mentioned above the bar.

The catalytic data obtained in this study for ceria-zirconia mixed oxides with an equimolar composition or nearly equimolar composition is compared with literature data (Fig. 8). We have restricted our comparison to data obtained under three-phase conditions without a water removal system. It is very difficult to compare catalytic activities under the same experimental conditions, as no standard testing protocol exists. Nevertheless, for each set of published data, the highest conversion reached versus

ceria-zirconia composition was selected. Activities were calculated from the parameters of the corresponding study (mass of catalyst and reaction duration). Obviously the FSP catalyst is far more active than any other catalyst reported ($6 \mu\text{mol} \cdot \text{s}^{-1} \cdot \text{g}^{-1}$), while the co-precipitated catalyst showed activities in the same order of magnitude as other good ceria-zirconia mixed oxides reported in the literature.

The unexpectedly high catalytic activity of the flame spray pyrolysis ceria-zirconia led us to investigate other ceria-based oxides prepared by flame spray pyrolysis. The second metal was selected among the best found by impregnation or co-precipitation methods, namely Zn, La and Nd. Ceria mixed oxides were obtained using the same process as for flame spray pyrolysis ceria-zirconia. The specific surface areas for these solids were around $95 (\pm 8) \text{ m}^2 \text{ g}^{-1}$ (E.S.I, Table 8S). The catalytic results are benchmarked against the flame spray pyrolysis ceria (Fig. 9). The addition of La, Nd and Zn significantly increased the activity compared to pure FSP ceria. This result confirmed the value of introducing a small amount of Zr, La or Nd into the ceria as previously reported for impregnated samples. Nevertheless, the activity gap compared to the co-precipitated samples was not as remarkable as it was for ceria-zirconia.

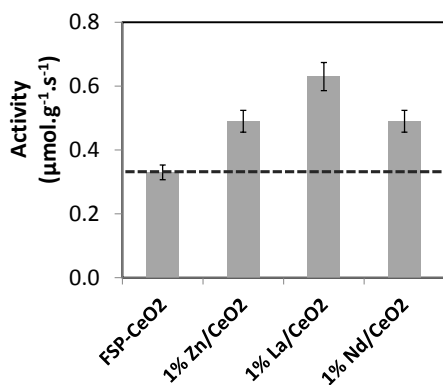


Fig. 9: Activities of flame-sprayed ceria-based oxides. The horizontal dashed line is a guide for the eyes. Dopants content are expressed in wt%.

4 Conclusions

The present work describes a robust method for measuring catalytic activity for DMC synthesis from methanol and CO₂ far from equilibrium conditions. This method made it possible to rank the activity of more than 60 catalysts which, to the best of our knowledge, is the largest consistent dataset yet reported. Different synthesis methods and compositions were tested. By selecting the most active composition of ceria-zirconia samples and further exploring different synthesis approaches, we found that the synthesis of mixed ceria-zirconia oxides by flame spray pyrolysis yielded the most active catalysts reported so far. We do not claim that other catalysts with higher activity could not exist, as the screening was of moderate size. On the contrary, we believe that better catalysts may exist with different Ce-Zr ratios, in particular Ce-rich compositions or solids that have undergone an optimized thermal treatment.

It is common to say that the structure of mixed oxides, especially the surface composition, strongly depends on the synthesis method and on the thermal treatment. We have observed that the addition of alumina yields better catalysts when it was added by co-precipitation, whereas a drop in activity was obtained by impregnation. We have also observed that for the latter method, high catalytic activities is obtained after a post-treatment at high temperature. Surprisingly, the catalytic activity of precipitated Ce_{0.88}Zr_{0.12}O₂ treated at different temperature is inversely correlated to its surface area. This suggests major modifications of the surface upon thermal treatment.

The activity of ceria-zirconia mixed oxides is about one order of magnitude higher when they are prepared by flame spray pyrolysis as opposed to by co-precipitation. The characterization of the structure by XRD or the texture by N₂ physisorption did not reveal significant differences that could account for such a difference in catalytic activities. More detailed investigations are required for the elucidation of structural features that are responsible for the high catalytic activity of mixed ceria-zirconia obtained by flame spray pyrolysis. This study will be published separately.

Acknowledgements

The work leading to these results received funding from the European Union Seventh Framework Program FP7-NMP-2010-Large-4, under grant agreement no 263007 (acronym CARENA). We thank Solvay and Johnson-Matthey for providing samples.

References

- 1 Y. Ono, *Appl. Catal. A Gen.*, 1997, **155**, 133–166.

- 2 E. A. Quadrelli, G. Centi, J.-L. Duplan and S. Perathoner, *ChemSusChem*, 2011, **4**, 1194–1215.
- 3 P. Tundo, L. Rossi and A. Loris, *J. Org. Chem.*, 2005, **70**, 2219–24.
- 4 S. Memoli, M. Selva and P. Tundo, *Chemosphere*, 2001, **43**, 115–21.
- 5 B. Schöffner, F. Schöffner, S. P. Verevkin and A. Börner, *Chem. Rev.*, 2010, **110**, 4554–81.
- 6 A. Arteconi, A. Mazzarini and G. Di Nicola, *Water, Air, Soil Pollut.*, 2011, **221**, 405–423.
- 7 M. Balaish, A. Kraysberg and Y. Ein-Eli, *Phys. Chem. Chem. Phys.*, 2014, **16**, 2801.
- 8 D. Delledonne, F. Rivetti and U. Romano, *Appl. Catal. A Gen.*, 2001, **221**, 241–251.
- 9 T. Sakakura and K. Kohno, *Chem. Commun. (Camb.)*, 2009, 1312–1330.
- 10 N. Keller, G. Rebmann and V. Keller, *J. Mol. Catal. A Chem.*, 2010, **317**, 1–18.
- 11 Q. Cai, B. Lu, L. Guo and Y. Shan, *Catal. Commun.*, 2009, **10**, 605–609.
- 12 E. Leino, P. Mäki-Arvela, V. Eta, D. Y. Murzin, T. Salmi and J.-P. Mikkola, *Appl. Catal. A Gen.*, 2010, **383**, 1–13.
- 13 B. a. V. Santos, V. M. Silva, J. Loureiro and A. Rodrigues, *ChemBioEng Rev.*, 2014, **1**, 214–229.
- 14 V. Eta, P. Mäki-Arvela, J. Wärn, T. Salmi, J.-P. P. Mikkola, D. Y. Murzin, J. Wärnå, T. Salmi, J.-P. P. Mikkola and D. Y. Murzin, *Appl. Catal. A Gen.*, 2011, **404**, 39–46.
- 15 M. Honda, S. Kuno, S. Sonehara and K. Fujimoto, *System*, 2011, **8511**, 365–370.
- 16 M. Honda, M. Tamura, Y. Nakagawa and K. Tomishige, *Catal. Sci. Technol.*, 2014, **4**, 2830.
- 17 J.-C. Choi, L. He, H. Yasuda and T. Sakakura, *Green Chem.*, 2002, **4**, 230–234.
- 18 C. Li and S. Zhong, *Catal. Today*, 2003, **82**, 83–90.
- 19 A. Dibenedetto, M. Aresta, A. Angelini, J. Ethiraj and B. M. Aresta, *Chemistry*, 2012, **18**, 10324–34.
- 20 A. H. Tamboli, A. A. Chaugule and H. Kim, *Chem. Eng. J.*, 2017, **323**, 530–544.

- 21 S. Huang, B. Yan, S. Wang and X. Ma, *Chem. Soc. Rev.*, 2015, **44**, 3079–3116.
- 22 H. J. Lee, W. Joe, J. C. Jung and I. K. Song, *Korean J. Chem. Eng.*, 2012, **29**, 1019–1024.
- 23 Y. Ikeda, M. Asadullah, K. Fujimoto and K. Tomishige, *J. Phys. Chem. B*, 2001, 10653–10658.
- 24 K. Tomishige, Y. Furusawa, Y. Ikeda, M. Asadullah and K. Fujimoto, *Catal. Letters*, 2001, **76**, 71–74.
- 25 K. Tomishige, T. Sakaihorii, Y. Ikeda and K. Fujimoto, *Catal. Letters*, 1999, **58**, 225–229.
- 26 K. Tomishige, Y. Ikeda, T. Saikahori and K. Fujimoto, *J. Catal.*, 2000, **192**, 355–362.
- 27 Y. Yoshida, Y. Arai, S. Kado, K. Kunimori and K. Tomishige, *Catal. Today*, 2006, **115**, 95–101.
- 28 C. M. Marin, L. Li, A. Bhalkikar, J. E. Doyle, X. C. Zeng and C. L. Cheung, *J. Catal.*, 2016, **340**, 295–301.
- 29 P. Unnikrishnan and S. Darbha, *J. Chem. Sci.*, 2016, **128**, 957–965.
- 30 S. Wang, L. Zhao, W. Wang, Y. Zhao, G. Zhang, X. Ma and J. Gong, *Nanoscale*, 2013, **5**, 5582–8.
- 31 I. Prymak, O. Prymak, J. Wang, V. N. Kalevaru, A. Martin, U. Bentrup and S. Wohlrab, *ChemCatChem*, 2018, **10**, 391–394.
- 32 M. Aresta, A. Dibenedetto, C. Pastore, C. Cuocci, B. Aresta, S. Cometa and E. De Giglio, *Catal. Today*, 2008, **137**, 125–131.
- 33 M. Aresta, A. Dibenedetto, C. Pastore, A. Angelini, B. Aresta and I. Pápai, *J. Catal.*, 2010, **269**, 44–52.
- 34 P. Kumar, P. With, V. C. Srivastava, K. Shukla, R. Gläser, I. M. Mishra and H. Turunen, *RSC Adv.*, 2016, **6**, 110235–110246.
- 35 H. Liu, W. Zou, X. Xu, X. Zhang, Y. Yang, H. Yue, Y. Yu, G. Tian and S. Feng, *J. CO₂ Util.*, 2017, **17**, 43–49.
- 36 H. J. Hofmann, A. Brandner, P. Claus, H. J. Hofmann, A. Brandner and P. Claus,

- Chem. Eng. Technol.*, 2012, **35**, 2140–2146.
- 37 M. Honda, M. Tamura, Y. Nakagawa, K. Tomishige, Y. Nakagawa, K. Tomishige, W. Wei, Y. Sun, J. P. Mikkola, T. Salmi and D. Y. Murzin, *Catal. Sci. Technol.*, 2014, **4**, 2830–2845.
- 38 B. Santos, C. Pereira, V. Silva, J. Loureiro and A. Rodrigues, *Appl. Catal. A Gen.*, 2013, **455**, 219–226.
- 39 P. Kumar, P. With, V. C. Srivastava, R. Gläser and I. M. Mishra, *J. Alloys Compd.*, 2017, **696**, 718–726.
- 40 R. Keiski, D. Ballivet-tkatchenko, R. Ligabue, L. Plasseraud, P. Richard and H. Turunen, *Catal. Today*, 2006, **115**, 80–87.
- 41 M. Honda, M. Tamura, Y. Nakagawa, K. Nakao, K. Suzuki and K. Tomishige, *J. Catal.*, 2014, **318**, 95–107.
- 42 R. Strobel, A. Baiker and S. E. Pratsinis, *Adv. Powder Technol.*, 2006, **17**, 457–480.
- 43 K. Wegner, B. B. Schimmoeller, B. B. Thiebaut, C. Fernandez and T. N. Rao, *Kona Powder Part. J.*, 2011, **29**, 251–265.
- 44 A. Auroux and A. Gervasini, *J. Phys. Chem.*, 1990, **94**, 6371–6379.
- 45 A. M. Maitra, *J. Therm. Anal.*, 1990, **36**, 657–675.
- 46 Y. Yoshida, Y. Arai, S. Kado, K. Kunimori and K. Tomishige, *Catal. Today*, 2006, **115**, 95–101.
- 47 D. Stošić, S. Bennici, V. Rakić and A. Auroux, *Catal. Today*, 2012, **192**, 160–168.
- 48 Z.-F. Zhang, Z.-W. Liu, J. Lu and Z.-T. Liu, *Ind. Eng. Chem. Res.*, 2011, **50**, 1981–1988.
- 49 W. J. Stark, L. Mädler, M. Maciejewski, S. E. Pratsinis and A. Baiker, *Chem. Commun.*, 2003, **38(4)**, 588–589.
- 50 W. J. Stark, M. Maciejewski, L. Mädler, S. E. Pratsinis and A. Baiker, *J. Catal.*, 2003, **220**, 35–43.
- 51 R. Di Monte and J. Kašpar, *J. Mater. Chem.*, 2005, **15**, 633–648.